Tight coupling of GPS-EGNOS and robot odometry with integrity provision

David Bétaille, Jérôme Soubielle, Mickael Crozes

Tight coupling of GPS-EGNOS and robot odometry with integrity provision

David Bétaille, *Laboratoire Central des Ponts et Chaussées*
Jérôme Soubielle, *M3Systems*
Mickael Crozes, *M3systems*

BIOGRAPHY

David Bétaille is a researcher in the Geolocalization Research Group of the LCPC, where his current activity relates to vehicles positioning by satellites systems combined with dead-reckoning and mapping. ADAS and in general road safety applications compose the research context of his lab. He received his PhD in 2004 for his investigations at University College London on phase multipath in kinematic GPS.

Jérôme Soubielle is a researcher and a project leader in the Radionavigation Unit of the M3Systems Company. His activities concern several aspects like the problem of GNSS interference or the hybridization of GNSS with inertial sensors. He received his PhD in 1999 at the University of Cergy Pontoise after a study on multipath mitigation.

Mickaël Crozes is a development engineer in the Radionavigation Unit of the M3Systems Company. His activities concern several aspects of ITS (Intelligent Transportation Systems) but also and mainly the development of post-processing and real-time radio-navigation software. His expertise covers several domains such as the knowledge of the MOPS standards, the use of EGNOS data servers (EMS, EDAS) and the implementation of hybridized systems.

INTRODUCTION

This article presents two different models for coupling GPS-EGNOS pseudo-ranges and Doppler measurements applicable in the context of a terrestrial vehicle, precisely a mobile robot used for unmanned transportation of persons in city centres, industrial or touristic resorts, multi-modal platforms…

The first approach is based on the most usual 3D predictive model used in navigation, assuming constant acceleration of the vehicle. The alternative approach assumes that the robot moves in its local tangent plane, which leads to the usual non-holonomic 2D predictive model.

These algorithms were proposed and developed during the CTS-SAT (Cybernetic Transport System - SATellite) project that aims at developing an innovative automated transport system based on satellite navigation coupled with additional sensors and to demonstrate the capability of GNSS-based guidance for such systems without need for an heavy ground infrastructure.

The CTS-SAT project was conducted by Robosoft in charge of the automatic vehicle production, M3Systems responsible of the radio-navigation algorithms and equipment, the « Laboratoire Central des Ponts et Chaussées » LCPC for their experience in inertial sensors and data fusion, Skylab Industries as a technical service provider, and the French attraction park « la Cité de l'Espace » in Toulouse as the test and validation site for the CTS-SAT concept

DESCRIPTION OF THE NAVIGATION MODELS

3D predictive model

The 11x1 state space vector x of the 3D model is defined by the position (X,Y,Z), velocity $(\dot{X},\dot{Y},\dot{Z})$ and acceleration $(\ddot{X},\ddot{Y},\ddot{Z})$ of the antenna in the Earth-Centred-Earth-Fixed (ECEF) frame, and the receiver clock bias and drift $c\Delta t$ and $c\Delta\dot{t}$:

$$x = \begin{bmatrix} X & Y & Z & c\Delta t & \dot{X} & \dot{Y} & \dot{Z} & c\Delta\dot{t} & \ddot{X} & \ddot{Y} & \ddot{Z} \end{bmatrix}^T$$

The (2m+2)x1 measurement vector y is defined by the pseudo-ranges and velocities (deduced from the Doppler frequency measurement Fd_i) and the horizontal velocity and vertical turn rate given by the on-board odometer and gyrometer:

$$y = \begin{bmatrix} \rho_1 & \cdots & \rho_m & \upsilon_1 & \cdots & \upsilon_m & V & \dot{\Psi} \end{bmatrix}^T$$

where, for each 1 ≤ i ≤ m (m is the number of tracked satellites):

$$\rho_i = \sqrt{\left[\left(X^i_{sat} - X\right)^2 + \left(Y^i_{sat} - Y\right)^2 + \left(Z^i_{sat} - Z\right)^2\right]} + c\Delta t$$

$$\upsilon_i = c\frac{Fd_i}{L_1} = -\frac{\left[\left(\dot{X}^i_{sat} - \dot{X}\right)\left(X^i_{sat} - X\right) + \left(\dot{Y}^i_{sat} - \dot{Y}\right)\left(Y^i_{sat} - Y\right) + \left(\dot{Z}^i_{sat} - \dot{Z}\right)\left(Z^i_{sat} - Z\right)\right]}{\sqrt{\left[\left(X^i_{sat} - X\right)^2 + \left(Y^i_{sat} - Y\right)^2 + \left(Z^i_{sat} - Z\right)^2\right]}} - c\Delta\dot{t}$$

with $\left(X^i_{sat}, Y^i_{sat}, Z^i_{sat}\right)$ the ith-satellite position in the ECEF frame, $\left(\dot{X}^i_{sat}, \dot{Y}^i_{sat}, \dot{Z}^i_{sat}\right)$ the ith-satellite velocity in the ECEF frame. c is light velocity and L1 is the GPS carrier frequency.

Atmospheric delays, as well as satellite clock terms, have been already removed from the pseudo-ranges, using either GPS standard models or EGNOS data.

The final components of the measurement vector are the horizontal velocity measurement V given by the odometer and the vertical angular rotation rate measurement ω given by the gyrometer.

The inertial measurement model is defined by the following equations where V_N and V_E are respectively the velocities according to North and East directions:

$$V = \sqrt{V_N^2 + V_E^2} \qquad \omega = \frac{\dot{V}_N V_E - \dot{V}_E V_N}{V_E^2 + V_N^2}$$

The lever arms between the odometer, the gyrometer and the GPS antenna have been taken into account.

The filtering process is a standard EKF algorithm [1] (Extended Kalman Filter). For each iteration step k, the following standard equations are applied:

Prediction: $\hat{x}_{k/k-1} = \Phi_{k-1}\hat{x}_{k-1/k-1}$

$$P_{k/k-1} = \Phi_{k-1} P_{k-1/k-1} \Phi_{k-1}^T + Q_{k-1}$$

Update: $\hat{x}_{k/k} = \hat{x}_{k/k-1} + K_k\left[y_k - h_k\right]$

$$P_{k/k} = \left(I - K_k H_k\right) P_{k/k-1}$$

with the filter gain K computed as follows:

$$h_k = h_x^{gps}\left(\hat{x}_{k/k-1}\right)$$

$$H_k = H_{gps}\left(\hat{x}_{k/k-1}\right) = \left(\frac{\partial h_x^{gps}(x)}{\partial x}\right)$$

$$K_k = P_{k/k-1} H_k^T \left[H_k P_{k/k-1} H_k^T + R_k\right]^{-1}$$

The prediction matrix Φ and its covariance matrix Q are determined by the prediction model, which is based on a Gauss-Markov process applied to the acceleration variable (refer to [1]). The prediction vector h of measurement and the projection matrix H between state vector and GPS and inertial measurement models are fully determined by the state vector and these models.

As concerns the satellite measurement noise model, the a priori pseudo-range standard deviations given by the EGNOS messages apply. Moreover, the velocity of the vehicle has been deduced from time stamped odometer pulses: the encoder resolution of the robot wheels (noted *step*) is so high that the standard deviation applicable to distance measurement ($step/\sqrt{6}$) is negligible. Last, for the gyrometer (a KVH fibre optic model here), it is accepted that a purely random walk model characterizes its noise, hence the turn rate standard deviation equals the manufacturer specified random walk ($0.083°/\sqrt{h}$) divided by $60\sqrt{Ts}$, where Ts is the filter time period.

Alternative 2D model

With the 2D model, the state space X contains the local plane co-ordinates of the robot, denoted x (for East) and y (for North), the heading angle θ measured from East to North, the altitude z, the receiver clock term ($c\Delta t$) and its drift ($c\dot{\Delta t}$).

Prediction: the predictive model is the next:

$$x_{k+1|k} = x_{k|k} + \Delta s_k \cos\left(\theta_k + \Delta\theta/2\right) + \nu_x$$

$$y_{k+1|k} = y_{k|k} + \Delta s_k \sin\left(\theta_k + \Delta\theta/2\right) + \nu_y$$

$$\theta_{k+1|k} = \theta_{k|k} + \Delta\theta_k + \nu_\theta$$

$$z_{k+1|k} = z_{k|k} + \nu_z$$

$$c\Delta t_{k+1|k} = c\Delta t_{k|k} + c\dot{\Delta t}_{k|k} Ts + \nu_{rckt}$$

$$c\dot{\Delta t}_{k+1|k} = c\dot{\Delta t}_{k|k} + \nu_{drift}$$

where Δs represents the variation in distance travelled between two sample times, and $\Delta\theta$ corresponds to a basic variation in heading over the same time period (Ts). With the gyrometer that yields rotational speed ω, it can be expressed that $\Delta\theta = \omega Ts$.

The 3 former equations make the classical non-holonomic 2D vehicle model used in robotics [2]. The lever-arm that should be applied to these equations in order to match the GPS positions used further is not written here.

These equations are nonlinear. Additive model noises ($\nu_x, \nu_y, \nu_\theta, \nu_z, \nu_{rckt}$ and ν_{drift}) and control noises (ν_{odo} and ν_{gyro} on Δs and ω respectively) are assumed to be centred, Gaussian and white, with variance-covariance matrices Q_{mod} and Q_{ctrl}.

The a priori covariance matrix $P_{k+1|k}$ is then given by:

$$P_{k+1|k} = A_k P_{k|k} A_k^T + B_k Q_{ctrl} B_k^T + Q_{\text{mod}}$$

where A and B represent the Jacobian matrices of evolution with respect to the state and control (partial derivatives of the prediction equations with respect to the state vector on the one hand and with respect to the control vector on the other, as calculated in the current state and control at time k).

Update: the predictive model is regularly updated when GPS raw measurements are available. In this version of the filter, only L1 pseudo-ranges have been used, with no Doppler.

To be applicable, satellite positions have to be converted from the ECEF (Earth Centred Earth Frame) to the local frame. Once this is done, the observation model for satellite i, with local co-ordinates $x_i y_i z_i$ is the next:

$$\rho_i = h_x^{gps}(X_{k+1|k}) = \sqrt{(x - x_i)^2 + (y - y_i)^2 + (z - z_i)^2} + \Delta t$$

Similarly as for the first model, the EKF gain and update equations apply. The observation matrix is fed with the partial derivatives of the pseudo-range equations with respect to the state vector. The satellite measurement covariance matrix is assumed to be diagonal and fed with the a priori pseudo-range standard deviations given by the EGNOS messages.

A test of consistency has been applied to every pseudo-range available for update. This consists in comparing the Mahalanobis distance (also called the Normalized Innovation Square) to the chi² threshold for m satellites and a given level of confidence, e.g. 99%. Only accepted pseudo-ranges are finally used to update the predicted state.

The set of parameters that characterize the noise levels of models and measurements requires special attention. Their tuning is made for a sample time (to which the gyrometer and odometer are sub-sampled) Ts of 0.1 s (i.e. 10 Hz). For the plane movement of the robot, one considers that 0.15 m is the standard error feasible within 0.1 s. The heading angle integration was assumed to be exact. As concerns the altitude, we used the same tuning as for the plane movement. Last, the receiver clock term and its drift were adjusted analyzing the corrections applied at update on various tests where we intentionally disabled the GPS observations. Standard error values of 0.1 m and 0.03 m/s at 10 Hz were found to be adequate.

Odometer and gyrometer noise models are those already depicted for the first model.

HPL computation

For the computation of the Horizontal Protection Level (HPL), the a priori pseudo-range standard deviations determined by the EGNOS messages are injected into the measurement covariance matrix R. Then the standard deviation upper bound σ_{maj} is determined according to the values of the Kalman estimated covariance matrix P related to the position. Then the HPL is given by:

$$HPL = \sigma_{maj} \times K\left(P_{MD}\right)$$

where $K(P_{MD})$ is the statistical protection factor depending of the desired misdetection probability for the considered application (it can be demonstrated that in the 2D navigation plan, the function K(.) is the Rayleigh inverse law).

Note that with the 2D model, we have proposed an *HPL-like* computation assuming that every a priori pseudo-range standard deviation equals 3 m.

On-board instruments and RT implementation

A low cost Ublox GPS chipset was used during the measurement campaign. It was implemented into the Safedrive receiver developed by M3systems and it was connected to a Novatel geodetic antenna GPS-702-GGL. During the measurement campaign, the Ublox raw GNSS and inertial data were collected. A Novatel receiver was also installed but only for ground truth purpose.

The Ublox receiver delivered data at 4Hz. In a previous study [3] using a post processing algorithm, the data were post processed in order to synchronize the inertial 10 Hz-data and the ran GNSS 4 Hz-data.

This new paper deals with the real time implementation of the algorithm, so the data are no longer synchronized. The output data are computed each 250 ms accordingly with the rate of the GNSS input raw data. The inertial 10 Hz measurements used at each computation are the latest ones resulting in an approximation of 100 ms maximum considering the low dynamic of the targeted application.

When no GNSS data input are available, the odometer and gyrometer 10 Hz measurements are used to compute a position but still at the GNSS receiver rate. During GPS outages, the inertial measurements are synchronised in real time.

The other main difference with [3] is that the odometry measurement data come from the Robosoft automatic vehicle and not from the LCPC test vehicle, with a much higher encoder resolution. Last, each time the vehicle is stopped, the gyrometer bias is measured.

APPLICATION IN FULL SCALE EXPERIMENT

Test site description

Both algorithms are applied to the same data set, a collection of trajectories performed in La Cité de l'Espace, Toulouse (Fig. 1). The environment, despite not being as severe as a urban canyon or an old city centre offers typical elevated buildings and structures from place to place, all along the different paths planned for the experiment. Multipath may happen that cause non-modelled perturbations in the set of observations (Fig. 3).

Fig. 1: The robot and on-board equipment on the test site

Reference trajectory

For data analysis purpose, the ground truth was provisioned by a high-grade IMU (Inertial Measurement Unit) composed of 3 accelerometer and 3 fibre optic gyroscopes (LandINS from IXSEA), coupled with the robot odometry and post-processed kinematic GPS solutions. Novatel DLV-3 dual frequency GPS receivers with geodetic antennas GPS-702-GGL were set-up on-board and on a local base station for that purpose.

Data set

22 runs were made, for a total duration of 2 hours, with various constellations. Each run corresponds to a return ride between points A and C (Fig. 2) with a way thought either points B1 or B2, this last being the closest travelled point with respect to the surrounding walls.

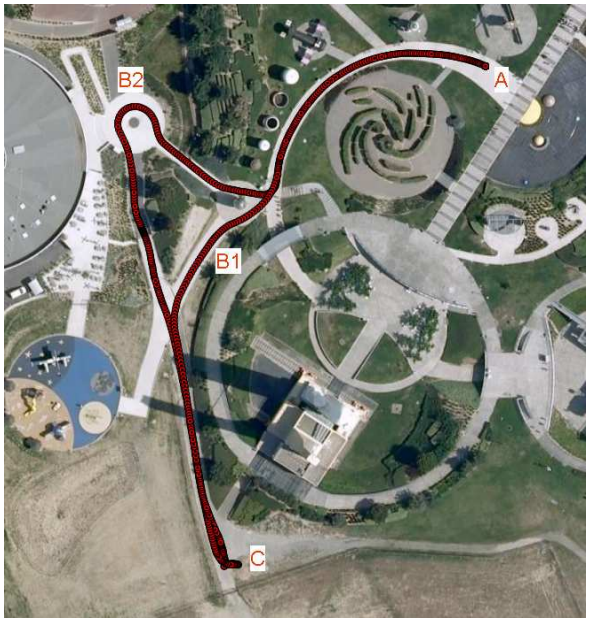

Fig. 2: Reference trajectory

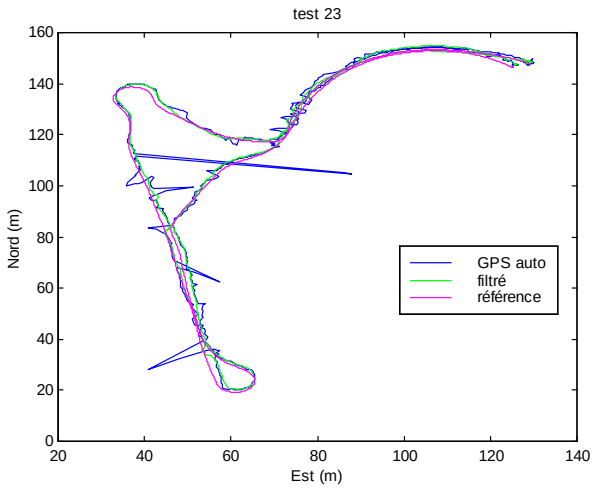

Fig. 3: Typical robot path with strong multipath effects on positioning

GNSS COMPUTATIONS MODES

Three different modes may be proposed to compute positioning solutions:

GPS-Standalone: no EGNOS correction is applied to the raw pseudo-ranges data and no integrity information is available.

GPS-EGNOS (SIS): the raw pseudo-ranges are corrected according to the EGNOS data received from the signal in space (SIS) from the geostationary satellites. This mode makes it possible integrity provision. Using the SIS EGNOS data, the environment of the receiver may cause several masks of the EGNOS service and interruption of the pseudo-ranges corrections and of the availability of the integrity information.

GPS-EGNOS (EMS): the EGNOS data are collected from the EGNOS Message Server (EMS) that allows us to simulate in post-processing the use in real time of EGNOS Data Access Service (EDAS). The EDAS server guarantees a full and continuous use of EGNOS when a real time connection between the server and the GNSS receiver is available. This connection can be realized through a GPRS or Wifi data link.

It is expected that in a free environment, the SIS and EMS modes will have a similar behaviour and availability whereas in an environment with low visibility of the EGNOS satellites, the results of the SIS mode will be similar to the GPS-Standalone mode.

Therefore, this article will deal only with the GPS-Standalone and GPS-EGNOS (EMS) modes, onto which we will apply (or not) odometer and gyrometer filtering.

The performance indicators of the proposed algorithms (further displayed in Stanford diagrams) are:
- The Horizontal Position Error (**HPE**) and its mean, 50% (or median) and 95% statistics. The HPE is the difference in the horizontal navigation plan between the reference trajectory and the computed position at the same time. The “95%” percentile indicates the maximum error level that is expected 95% of the time
- The Horizontal Protection Level (**HPL**) and its mean, 50% (or median) and 95% statistics
- The Misleading Information (**MI**) rate, which is the time percentage when the signal integrity is not achieved: (HPE>HPL)
- The Near Misleading Information (**NMI**) rate, which is the time percentage when the error is near the protection level: (HPL>HPE>0.75 HPL)
- The **Safety index,** which is the time percentage when there is no MI or NMI: (HPE<0.75 HPL).

GPS-STANDALONE

The following figures (Fig. 4, Fig. 5 and Fig. 6) present the performances of the 2 algorithms along with a least-squares (LS) epoch per epoch solution using the GPS-Standalone mode. These results were obtained using the raw GNSS data from the Ublox chipset with no EGNOS corrections.

All the results of the 22 runs were concatenated into a single time series in order to display the HPE.

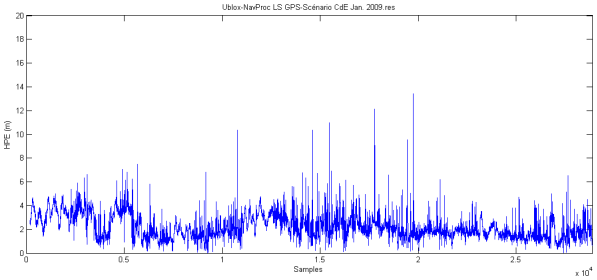

Fig. 4: LS Algorithm – GPS – Ublox chipset

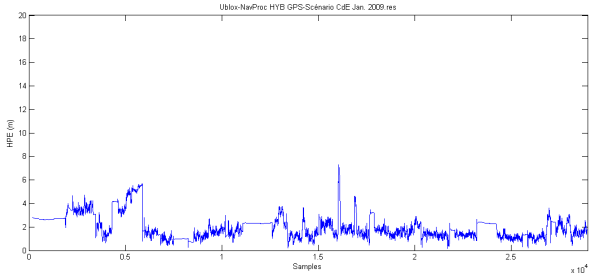

Fig. 5: 3D model filtering – GPS – Ublox chipset

On the following Fig. 6, the 2D model filtering provides also an HPL-like indicator that was not implemented for the 2 others. This could be easily done as the only hypothesis is a unique and constant a priori pseudo-range standard deviation of 3 m.

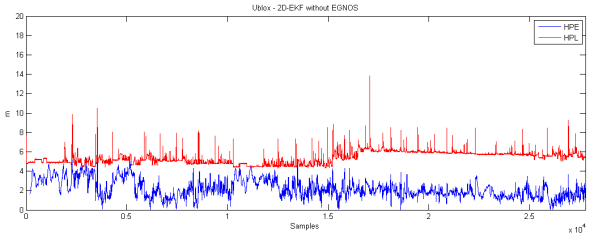

Fig. 6: 2D model filtering – GPS – Ublox chipset

The following Tab. 1 summarizes the statistics of the 3 algorithms and makes it possible a comparison of their performances. Maximum errors, already visible on Fig. 3, are eliminated.

Performances		**LS**	**3D-model**	**2D-model**
HPE (m)	Mean	2.21	1.96	2.19
	50%	2.00	1.67	1.99
	95%	3.98	3.99	3.93
	Max	13.40	7.31	6.06

Tab. 1: GPS-Standalone – Ublox chipset

On Tab. 1, the LS maximum error value was obtained filtering the aberrant values according to the simple measurement of the velocity based on two consecutive epochs. When this value is above a threshold value of 100 m/s, the PVT solution is not considered into the statistics of Tab. 1. According to this test, the most important errors observed on Fig. 3 are no longer taken into account and the maximum value is only 13.40 m. For the other algorithms, this test was not necessary but the results demonstrate that the maximum error values are nevertheless improved.

Tab. 2 demonstrates that the simple hypothesis about the constant a priori pseudo range standard deviation protects quite well the system with a very low MI rate. This chosen constant value seems to properly take into account possible local errors considering the test environment. Of course, in a more severe environment like in urban canyons, the choice of this constant value shall be reviewed.

HPL-like availability	100%
Mean	5.53
50%	5.48
95%	6.52
Safety Index	92.57%
Near MI	7.78%
MI	0.05%

Tab. 2: GPS-Standalone – 2D model – Ublox chipset

GPS-EGNOS (EMS)

This section shows the performances in terms of position and integrity of the algorithms with EGNOS data. Using the EMS files, it is expected that the EGNOS data are 100% available However, for the measurements performed during this study, the measured EGNOS availability was equal to 99.25%. The 0.75% EGNOS unavailability can be explained by the following causes:

- Some missing data in the EMS EGNOS files (data from only one EGNOS satellite were used)
- EGNOS mode can be disabled by our algorithms in case of partial missing data. Our set-up is detailed next.

No assessment of the distribution between the two potential causes was performed.

Concerning our algorithms set-up, let us mention that:

- When the EGNOS data applicable to one satellite are available, the corresponding pseudo-range is always corrected.
- When N (with N≥4) pseudo-ranges are EGNOS corrected and P are not, only the N satellites are used to compute the position. The other satellites are excluded from the position computation. The HPL protection level is computed in accordance with the EGNOS characterisation of the N pseudo-range errors (EGNOS standard deviations).
- When N (with N<4) pseudo-ranges are EGNOS corrected and P are not, the N+P pseudo-ranges are used to compute the position. The EGNOS mode is considered as not available.

The following figures (Fig. 7, Fig. 8 and Fig. 9) present the performances of the 3 algorithms using EGNOS. These results were obtained using the GNSS data from the low cost Ublox chipset with EGNOS corrections when available. The statistics about the integrity are computed (Tab. 3) on the epochs where EGNOS data are available. As a consequence, the sum of the Safety percentage, Near-MI and MI percentages is 100%.

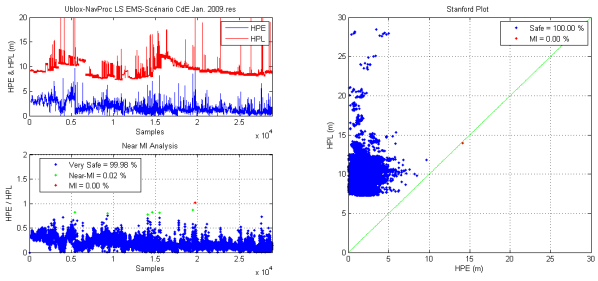

Fig. 7: LS Algorithm – GPS-EGNOS – Ublox chipset

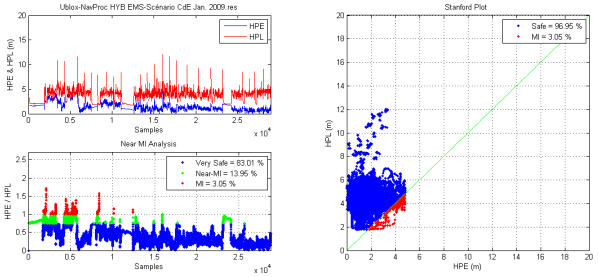

Fig. 8: 3D model filtering – GPS-EGNOS – Ublox chipset

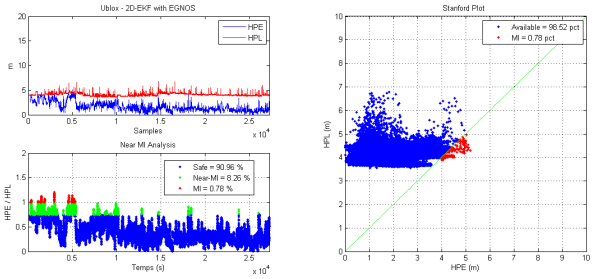

Fig. 9: 2D model filtering – GPS-EGNOS – Ublox chipset

On the above figures, the same $K(P_{MD})$ statistical protection factor was applied to generate the Horizontal Protection Level, the standard deviation upper bound σ_{maj} being obtained either from least-squares or Kalman filters output variance matrixes.

The integrity performances and statistics show that the Kalman filters (2D and 3D models) generates lower protection levels compared to the LS algorithm. Indeed, the MI rate that is obtained with the 3D-model equals a few percent (Tab. 3), whereas the one of the 2D-model is just less than 1%.

In order to reduce the number of MI, we suggest that a gain be applied to adapt the HPL formula. This formula is justified in the case of the LS algorithm where two consecutive samples can be assumed to be independent. In the case of the EKF algorithms this hypothesis is no longer true, because of the predictive model.

Therefore, a gain on the HPL protection level was assessed in order to minimize the number of MI without increasing too much the HPL. Next figure (Fig. 10) shows the integrity of the 3D-model with an adjustment of 1.25 on the protection level. Note that this gain factor has only an impact on the HPL but of course not on the HPE. No gain was applied on the 2D-model algorithm since it presents a low MI rate with the same HPL formula as the LS algorithm.

In conclusion, the filtering models and settings of the different variances used for prediction have an impact on the protection level, with a trade-off to be balanced between the GNSS observations and the inertial sensors.

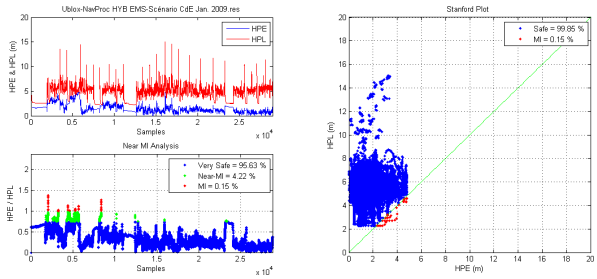

Fig. 10: 3D model filtering-GPS-EGNOS (EMS)- Ublox chipset + HPL gain

The following table summarizes the statistics of the 3 algorithms (+ HPL gain on the 3D-model) and allows the reader to compare their performances.

Performances		LS	EKF-3D	EKF-3D + HPL gain	EKF -2D
HPE	Mean	1.66	1.50		1.64
	50%	1.40	1.31		1.41
	95%	3.60	3.39		3.56
	Max	14.15	4.81		5.19
HPL	Mean	9.37	3.81	4.75	4.11
	50%	9.03	4.01	5.01	4.04
	95%	11.93	5.42	6.77	4.69
Safety Index (%)		99.98	83.0	95.63	90.96
Near MI (%)		0.02	13.95	4.22	8.26
MI (%)		0.00	3.05	0.15	0.78

Tab. 3: GPS-EGNOS (EMS) – Ublox chipset

For each algorithm, the mean, median and 95% errors are improved compared to the GPS-Standalone mode, demonstrating the effects of the EGNOS corrections. The maximum error is also reduced, except with the LS algorithm, which indicates a certain sensitivity of our simple velocity test, obviously not as robust and efficient as the more complete statistical tests performed by the Kalman filters.

CONCLUSIONS

As already stated in [3] with the initial tests at la Cité de l'Espace, the usefulness of an additional instrumentation (odometer and gyrometer) is demonstrated, compared to the GNSS solution. Not only does it help to bridge the GNSS outages, due to satellites masking, but also it statistically reduces the positioning error, reducing particularly its maximum in case of outlier occurrence. On this test site, fault detection and exclusion on pseudo-ranges are efficient, which explains why the filter shows a satisfactory general behaviour. Another point is noticeable: contrary to the least-squares algorithm, it is still possible with a filter to detect and exclude a faulty pseudo-range in a set of 4 satellites or less.

The filter modelling differences have no strong influence, but the most standard update 3D model that uses Doppler has a certain advantage as concerns the output error, respect to the non-holonomic robot model that does not.

As concerns EGNOS, its advantage is also shown: one notices EGNOS improvement in the least-squares algorithm and also in the EKF filters. Note that the EMS data server was used, to avoid any trouble with geo-satellite visibility. We think that this solution is valuable and reasonably feasible while communicating vehicles become a standard.

MOPS integrity computation (for standalone GPS) has been generalized to the EKF formalism in this study and an HPL has been derived. The method still needs to be consolidated, but it already achieves reasonable HPL with only few misleading information (MI) occurrences (a few percent). EGNOS pseudo-range standard deviations were used. When they were not available (i.e. without EGNOS), the proposed HPL-like computation, under the assumption of 3 m error level, gives also acceptable result. Moreover, this HPL-like is still delivered using the gyro and odometer error models during GNSS outages.

The results obtained with the LS algorithm demonstrated that very few (around 1/1000) loss of integrity MI are observed (Fig. 3) and that the maximum errors can be somehow sorted out by a simple velocity estimation based on two consecutive output. As concerns these outliers, the proposed Kalman filters prove to be more efficient and robust than this simple test. Nevertheless, the filters present some MI, which cannot be explained by the environment only. The settings of the 2D and 3D model algorithms, mainly on the prediction model covariance, seem to be optimistic and generate this MI percentage by providing rather low HPL levels. The settings could be optimized to guarantee a full integrity of the navigation system.

Last, but not least, these results have limited applicability to other test conditions in term of integrity. Actually, under more severe propagation environment, MI would probably increase significantly with the parameters adjusted for this data set only.

As concerns possible applications in autonomous transportation, the current performances do not meet our specification requirement at la Cité de l'Espace (with decimetre accuracy level typically because of the width of the Robucab vehicle compared to the width of the fire lane). This still suppose that RTK (real-time kinematic) GPS is operated on the area, as well as minimal additional dead-reckoning [4]. Nevertheless, other applications with less constraint are foreseen.

ACKNOWLEDGEMENTS

This research investigation has been carried out in the frame of the national programme ULISS of the Ministère de l'Economie, de l'Industrie et de l'Emploi in France, in the CTS-Sat project (Cybernetic Transportation Systems by Satellites).

The authors thanks go to all partners of this project, its leader Robosoft, M3S, the LCPC, Skylab, and last but not least, la Cité de l'Espace in Toulouse, where full scale tests and final demonstrations were carried out in January 2008, January and October 2009.

REFERENCES

[1] The Global Positioning System & Inertial Navigation. J.A. Farrell, M. Barth. Mc Graw Hill, 1999

[2] D. Bétaille, "GYROLIS: Post-processing of vehicle localization software via GPS - gyrometer - odometer coupling". Bulletin des Laboratoires des Ponts et Chaussées, No. 272, pp. 75–87, 2008

[3] EGNOS and MEMS sensors tight hybridization for automatic transport systems. J. Soubielle (M3systems), D. Bétaille (LCPC), W. Vigneau (M3systems). Conference NAVITECH. Dec 2008.

[4] Real-time 2D localization of a car-like robot using dead-reckoning and GPS, with satellite masking prediction, E. Lucet, D. Bétaille, D.-F. Nahimana, M. Ortiz, D. Sallé, J. Canou, Workshop GDR Robotique : Localisation Précise pour les Transports Terrestres, Paris, LCPC, 16 juin 2009, INRETS éditions.